A Bioinspired Model for Copper Monooxygenase: A Direct Aromatic Hydroxylation Using O_2

Ramamoorthy Ramasubramanian,[a,b] Karunanithi Anandababu,[a,b] Mukesh Kumar[c] and Ramasamy Mayilmurugan*[a,d]

[a]Department of Chemistry, Indian Institute of Technology Bhilai, Bhilai, Durg 491002, Chattisgarh India. E-mail: murugan@iitbhilai.ac.in
[b]Department of Chemistry, National Sun Yat-sen University, Kaohsiung, 80424, Taiwan.
[c] Radiation Biology and Health Sciences Division, Bhabha Atomic Research Centre, Mumbai, Maharashtra 400 085, India.

[d]Department of Bioscience and Biomedical Engineering, Indian Institute of Technology Bhilai, Bhilai, Durg 491002, Chattisgarh India.

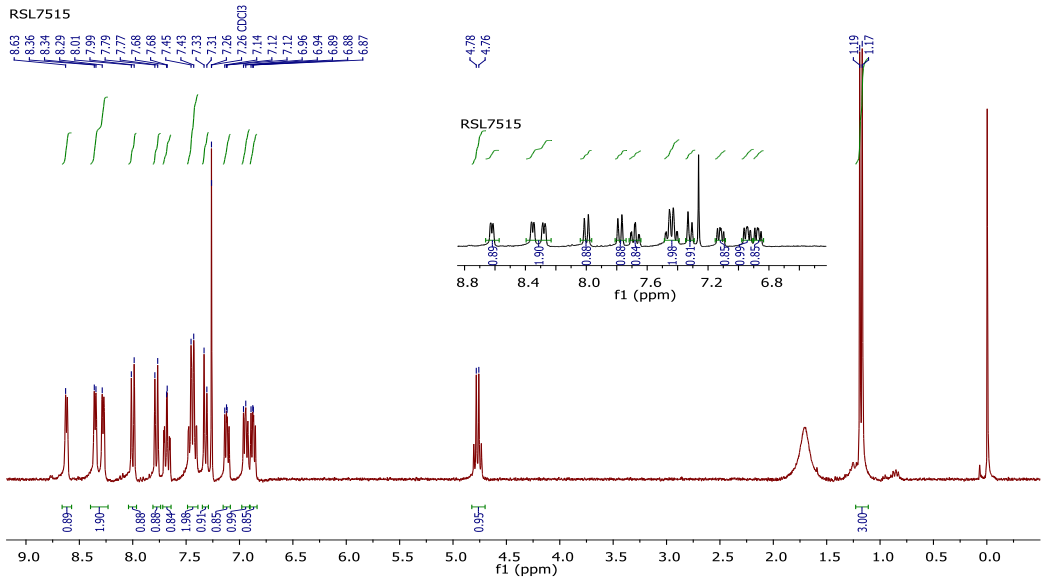

Figure S1. ^{1}H-NMR of 1,1,2-tri(pyridin-2-yl)propan-1-ol (**L1)** in $CDCl_3$.

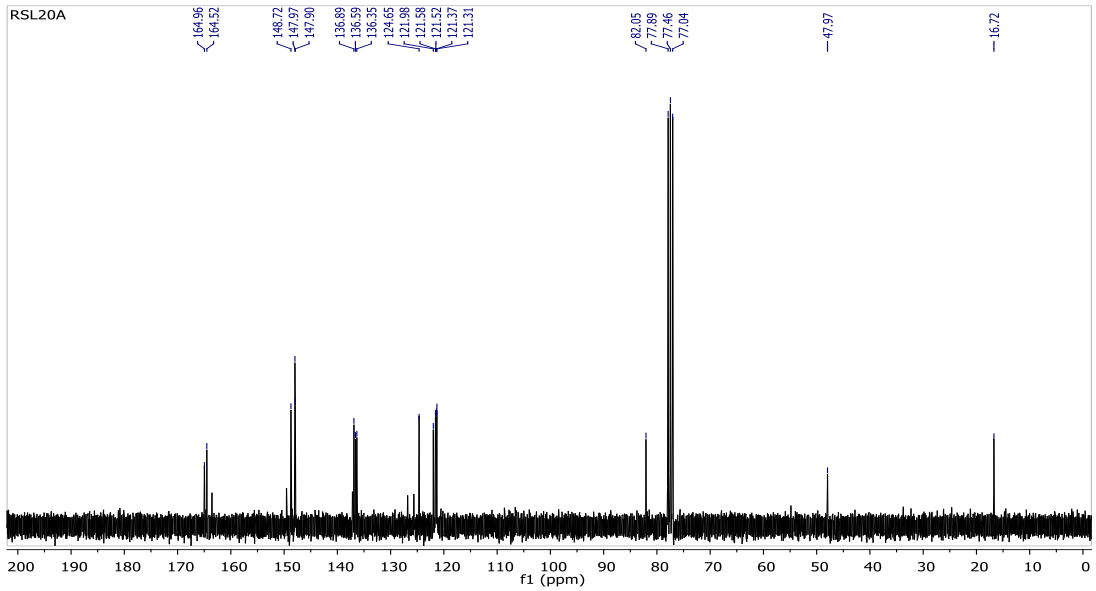

Figure S2. ^{13}C-NMR of 1,1,2-tri(pyridin-2-yl)propan-1-ol (**L1**) in $CDCl_3$.

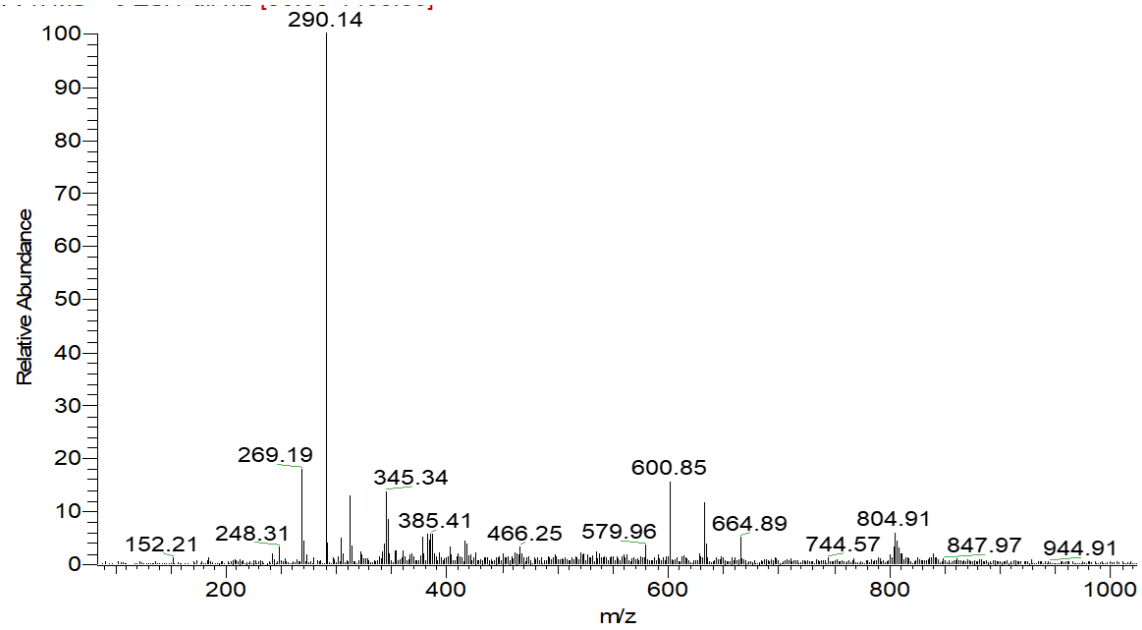

Figure S3. ESI- MS of L in CH_3OH. (290.14 corresponds to M-1 peak of ligand)

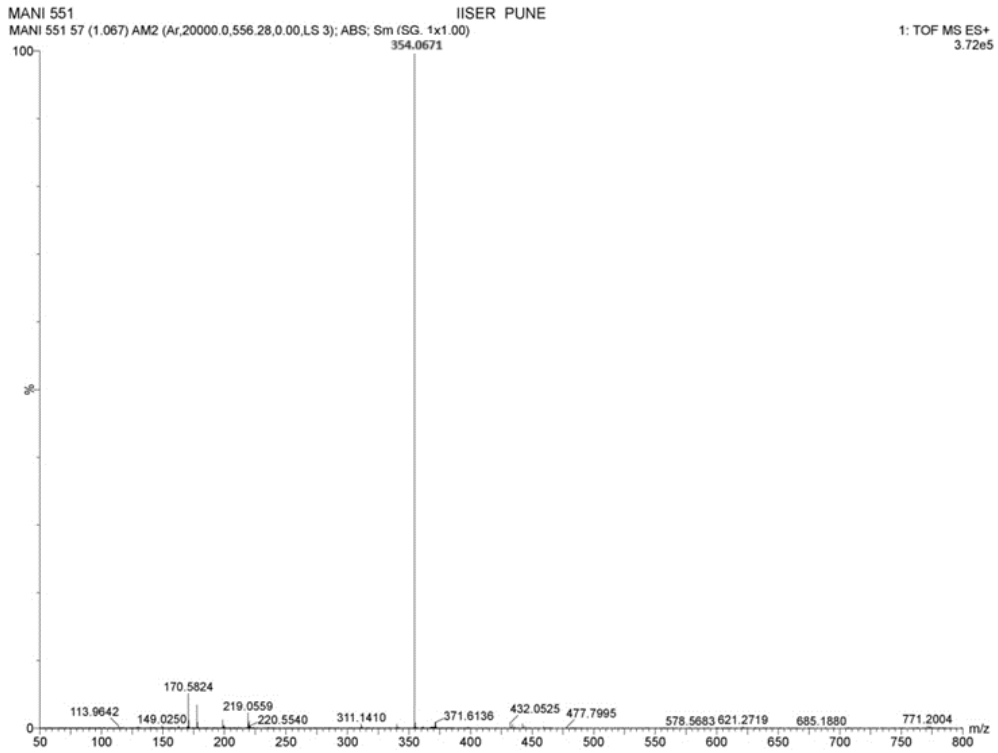

Figure S4. HRESI- MS of $[Cu^{I}(L)(CH_3CN)]CF_3SO_3$ (**1**) in CH_3CN.

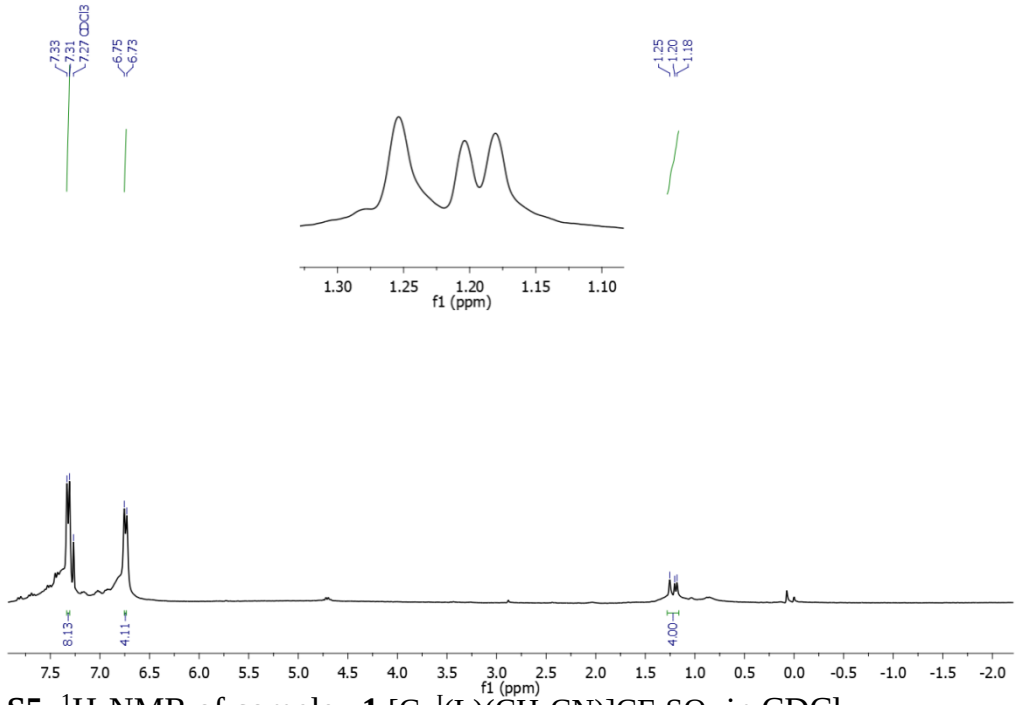

Figure S5. ^{1}H-NMR of complex **1** $[Cu^{I}(L)(CH_3CN)]CF_3SO_3$ in $CDCl_3$.

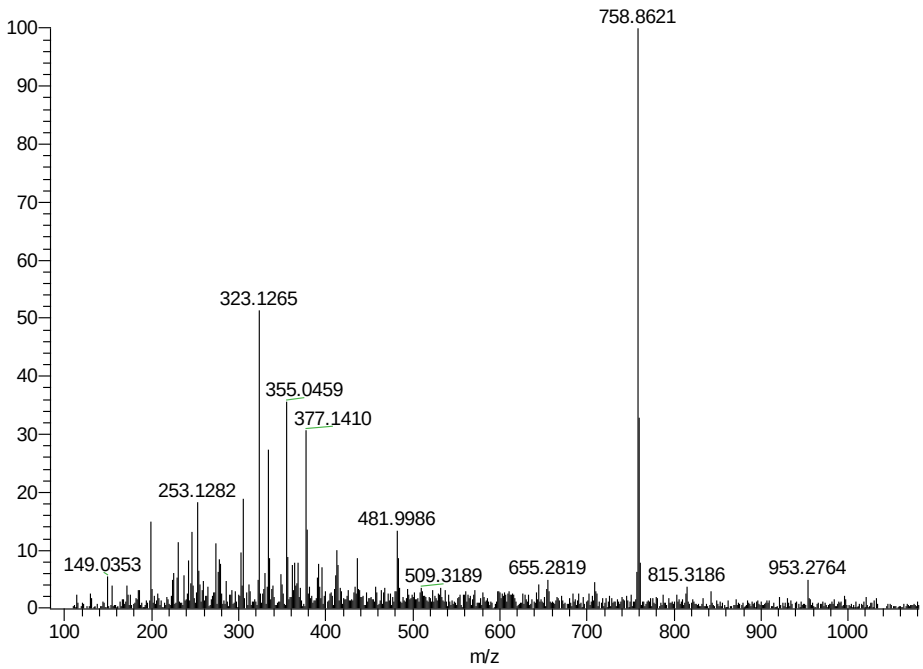

Figure S6. HRESI- MS of $[(Cu^{II}L)(Cu^{II}L\ H)(SO_3CF_3)_2]\cdot CF_3SO_3$ (**2**) in CH_3CN.

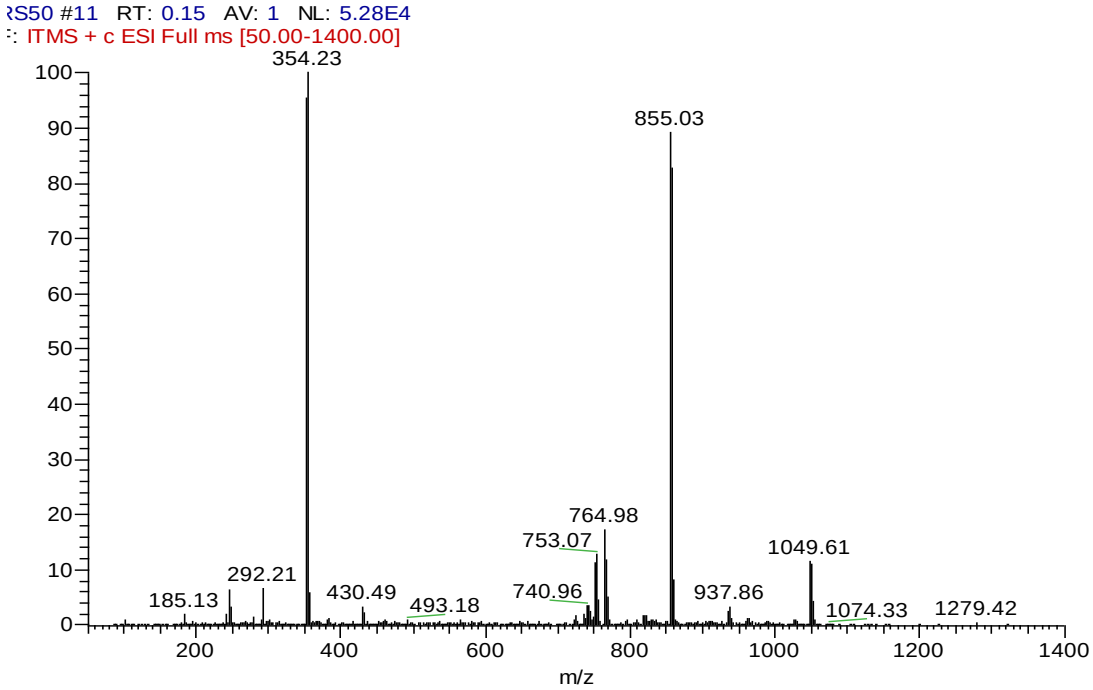

Figure S7. ESI- MS of $[(LCu^{II})_2(SO_3CF_3)_2]$ **3** in CH_3CN.

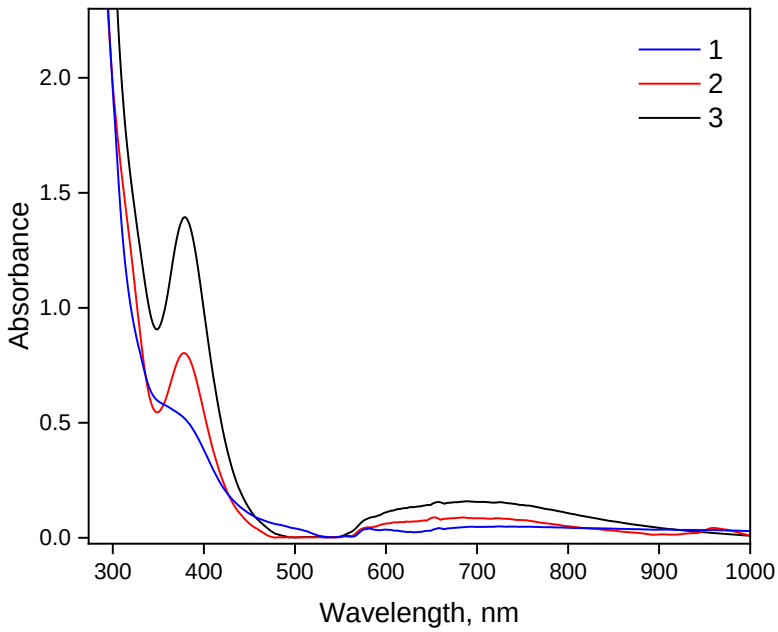

Figure S8. Electronic spectra of **1** (6×10^{-3} M) (blue), **2** (red), and **3** (black) (1×10^{-3} M) in acetonitrile at 25 °C.

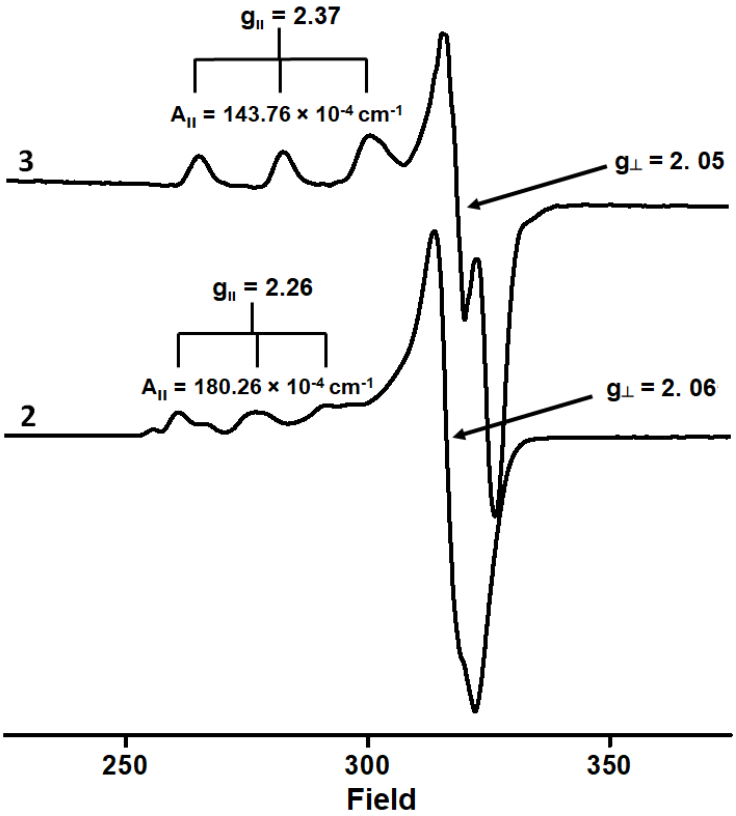

Figure S9. EPR spectra for **2** and **3** in DMF/CH_3CN mixture at 70 K.

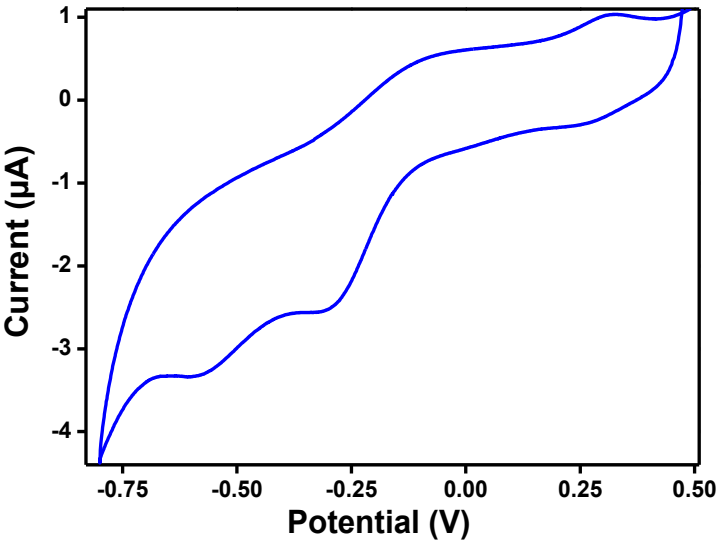

Figure S10. Cyclic voltammogram of **3** (1×10^{-3} M) in acetonitrile at 25 °C under N_2. Supporting electrolyte: 0.5 M TBAP; Reference: Ag/Ag^+; working electrode: Pt-sphere; Counter electrode: Pt wire.

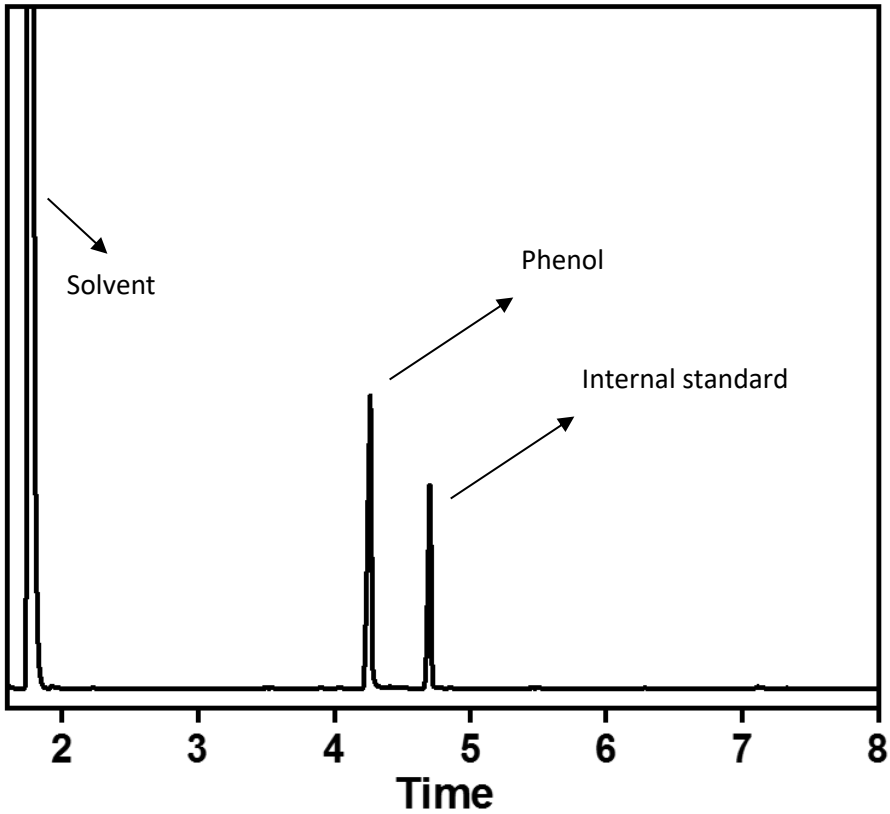

Figure S11. GC-MS chromatogram of the phenol in the presence of nitrobenzene as an internal standard.

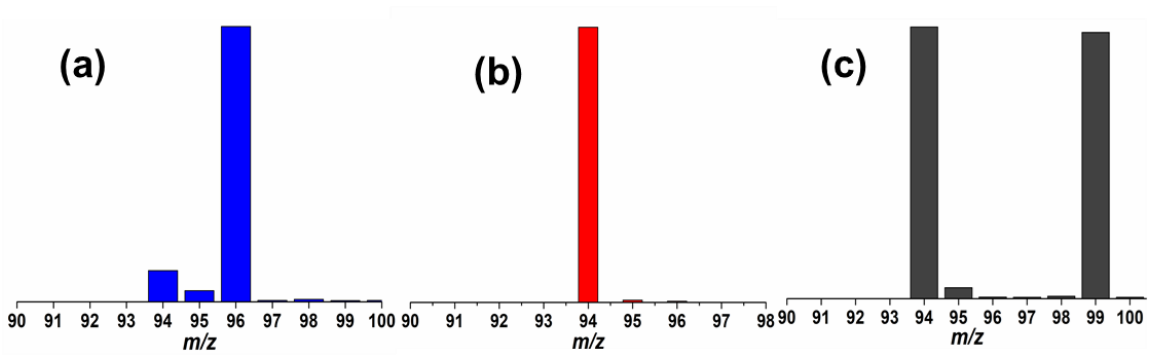

Figure S12. Isotopic studies for the benzene hydroxylation of **1** using $H_2{}^{18}O_2$ (a); benzene hydroxylation in presences of $H_2{}^{18}O/H_2O_2$ (b); representative figure of KIE studies with C_6H_6/C_6D_6 (1:1) in H_2O_2 at 60 °C (c).

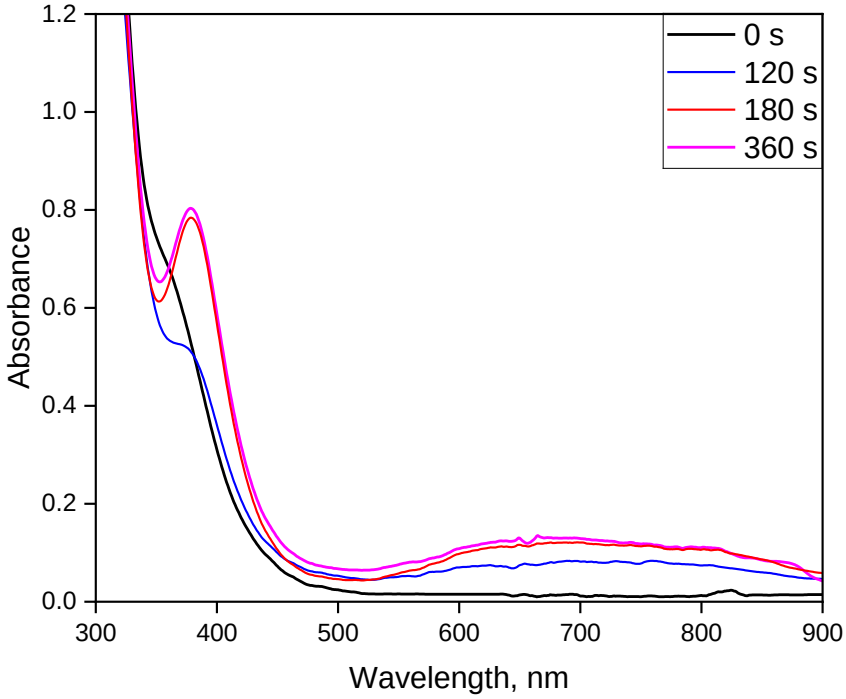

Figure S13. Electronic spectral changes for the reaction of **1** (7×10^{-3} M) with 2 equivalents Et_3N and O_2 purged at -20 °C in acetonitrile.

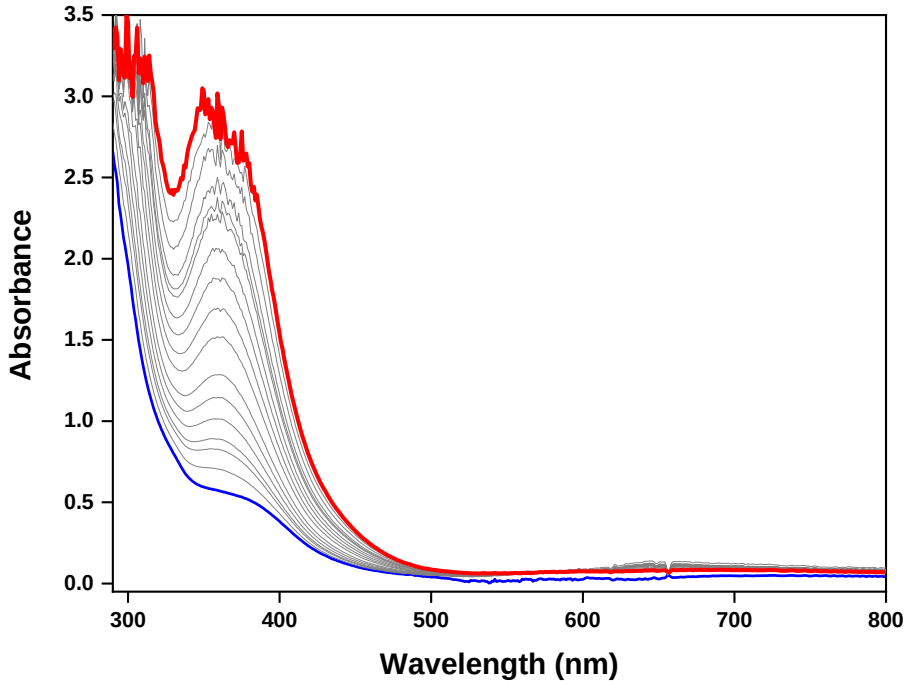

Figure S14. Electronic spectral changes for the reaction of complex **1** (5×10^{-3} M) with 2 equivalent Et_3N and 10 equivalent of H_2O_2 (30%) at 25 ˚C in dry acetonitrile.

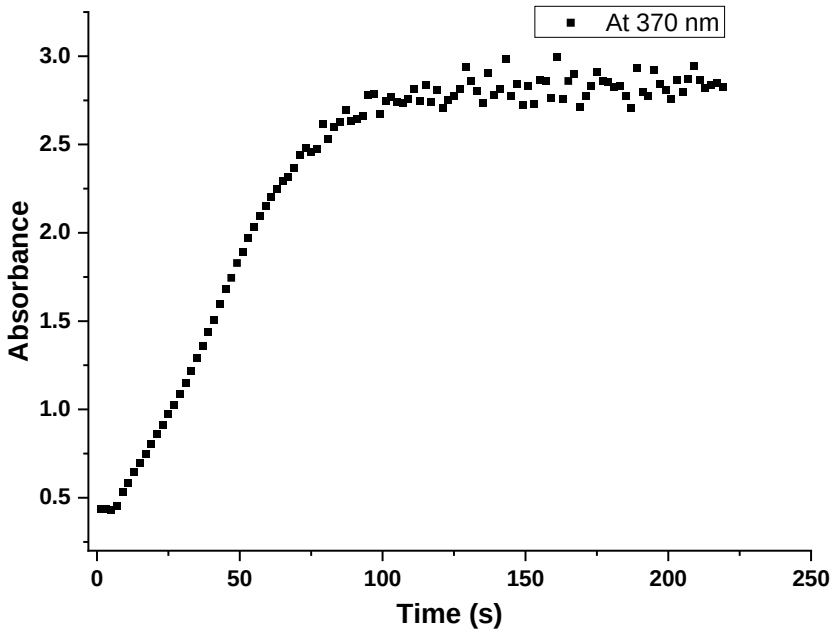

Figure S15. Plot of time vs. absorbance (370 nm) for the reaction of complex **1** with 2 equivalent Et_3N and 10 equivalent of H_2O_2 (30%) at 25 ˚C in dry acetonitrile

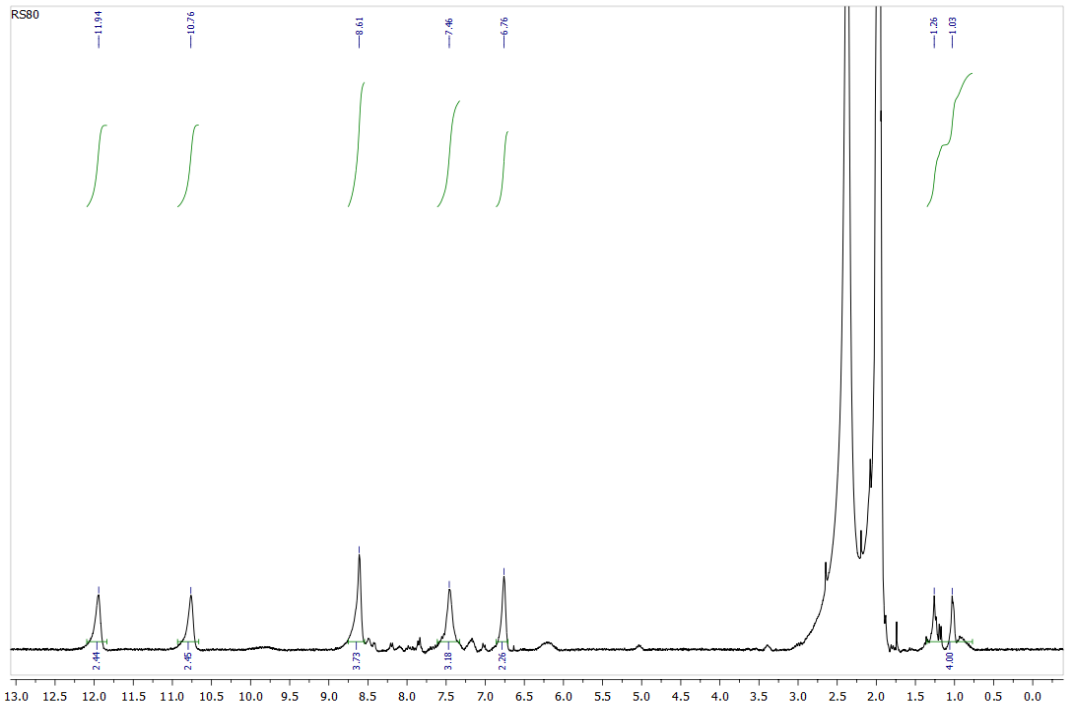

Figure S16. ^{1}H-NMR of **1** with H_2O_2; broadness and shift in NMR due to Cu-peroxo species (CD_3CN).

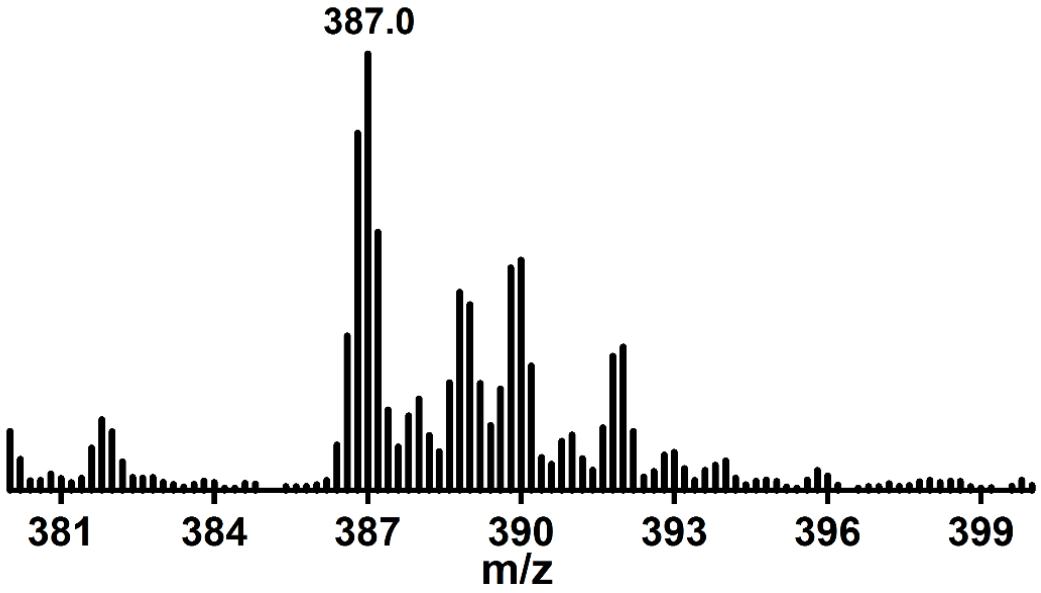

Figure S17. ESI-MS of complex **1** with 2 equivalents of Et_3N and 10 equivalent of $H_2{}^{16}O_2$.

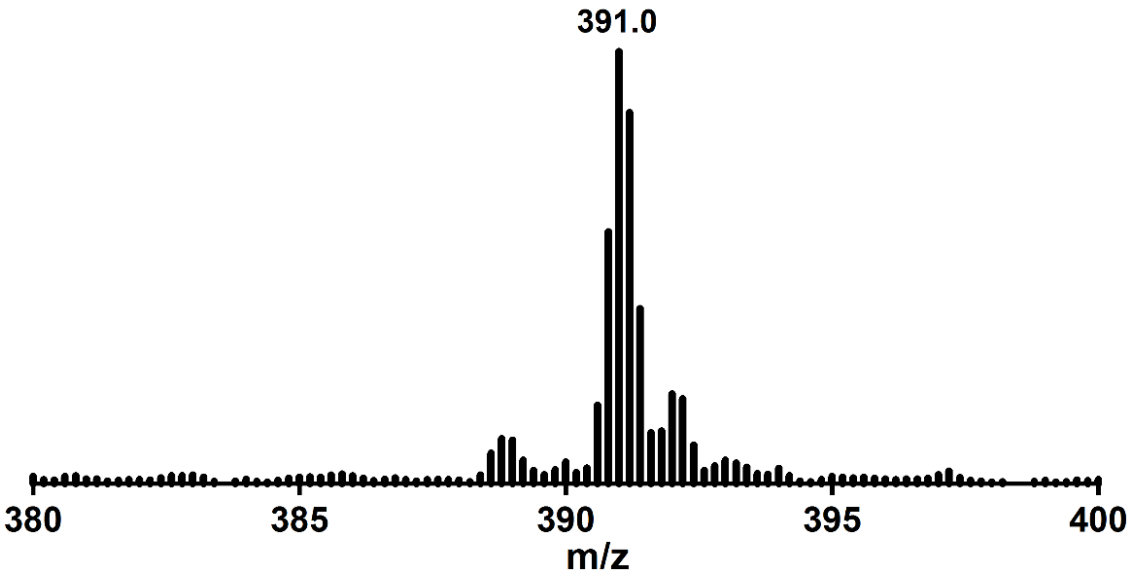

Figure S18. ESI-MS of complex **1** with 2 equivalents of Et_3N and 10 equivalent of $H_2{}^{18}O_2$.

a)

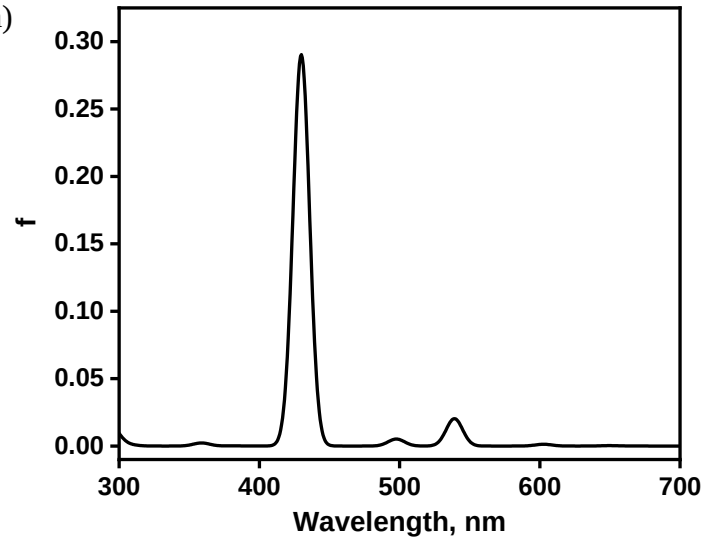

b)

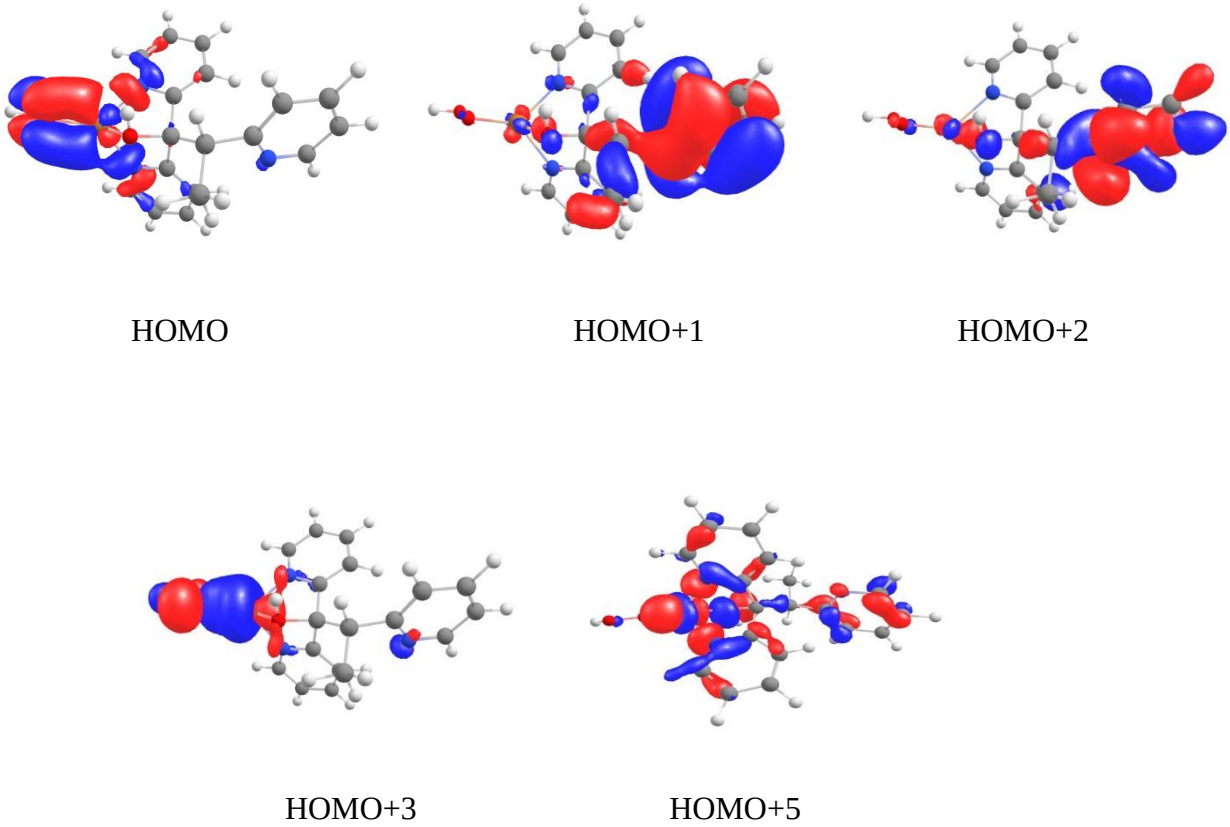

Figure S19. (a) Calculated electronic spectra of $[(L)Cu^{II}\text{-}OOH]^{+}$ by using TDDFT; (b) the molecular orbitals showing the transition involved in the electronic spectra of $[(L)Cu^{II}\text{-}OOH]^{+}$ for a peak at 429 nm by time-dependent DFT of $[(L)Cu^{II}\text{-}OOH]^{+}$ showed 429 nm which was responsible for five molecular orbital transitions such as HOMO+1 → HOMO, HOMO+2 → HOMO, HOMO+3 → HOMO and HOMO+5 → HOMO.

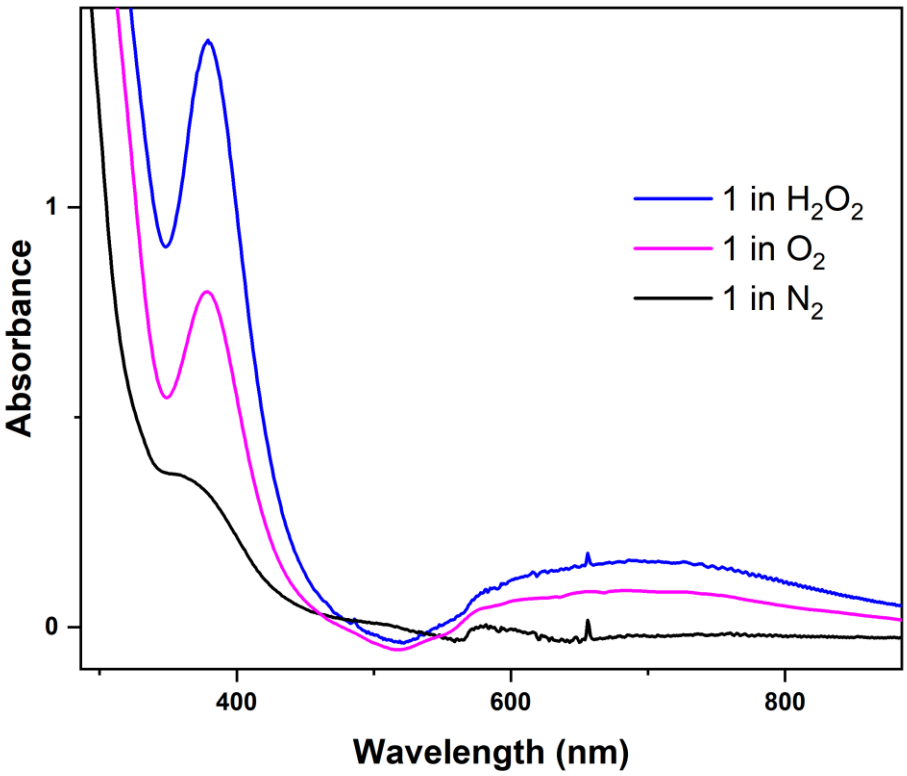

Figure S20. Electronic spectral changes for the reaction of **1** (5×10^{-3} M) in N_2 (black); spectral trace of **1** with 2 equivalents Et_3N and saturated O_2 (red) and spectral trace of **1** with 2 equivalents Et_3N and 10 equivalent of H_2O_2 (blue) at -20 °C in acetonitrile.

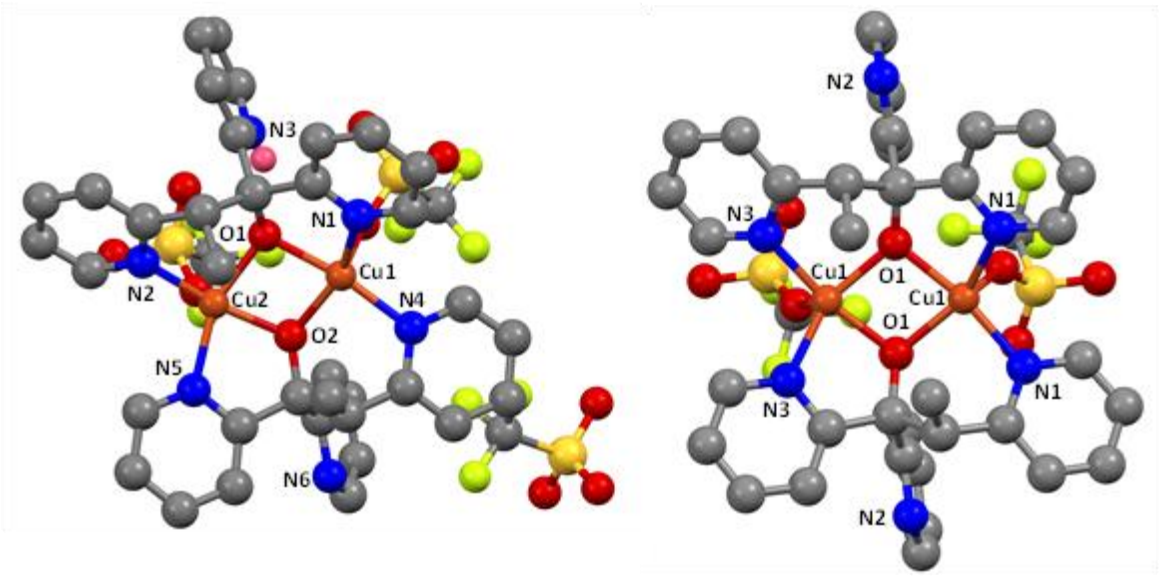

Figure S21. Molecular structures of **2** (left), and **3** (right). (Pov-ray figures drawn from 50% probability factor of thermal ellipsoids). For clarity, the hydrogen atoms and other counter ions are omitted.

a)

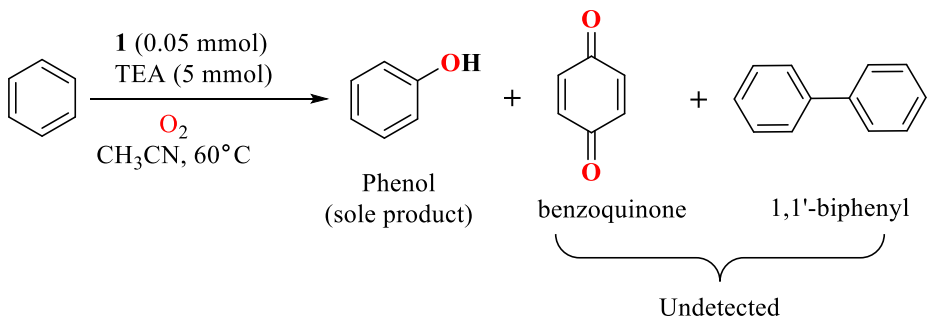

b)

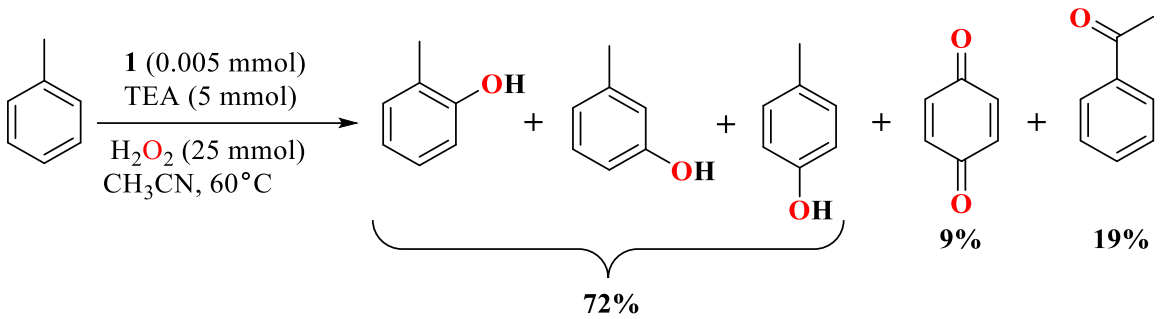

Scheme S1. Benzene and toluene hydroxylation using Copper(I) complex **1**.

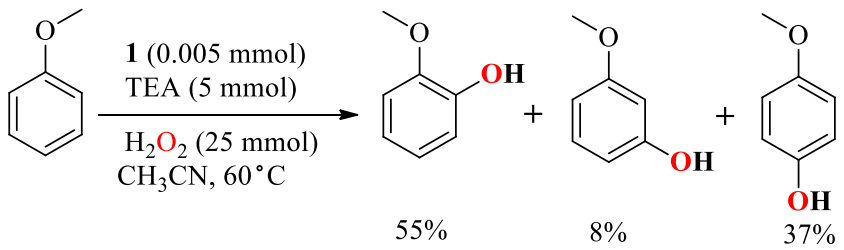

Scheme S2. Anisole hydroxylation using Copper(I) complex **1**.

Table S1. Crystal Data and Structure Refinement for complexes **2** and **3**

	2	**3**
Formula	$C_{39}H_{33}Cu_2F_9N_6O_{11}S_3$	$C_{38}H_{34}Cu_2F_6N_6O_8S_2$
Fw	1156.00	1007.94
Cryst system	Orthorhombic	Orthorhombic
Space group	$Pca2_1$	$C222_1$
Temperature	293(2) K	293(2)
a/Å	27.7616(6)	16.3112(4)
b/Å	10.1552(2)	17.5527(5)
c/A^0	16.5696(3)	14.4401(3)
$\alpha/^0$	90	90
$\beta/^0$	90	90
$\gamma/^0$	90	90
Volume/$Å^3$	4671.38(16)	4134.28(18)
Z	4	4
ρ_{calc} (mg/mm^3)	1.644	1.619
μ/mm^{-1}	3.275	2.978
F(000)	2333.2	2042.3
Reflection collected	12880	5526
Goodness-of-fit on F^2	1.087	1.148
$R1^a$	0.0751	0.0826
$wR2^b$	0.1902	0.2584

$^aR1=\Sigma\,||Fo|-|Fc||/\Sigma|Fo|$, $^bWR_2=\Sigma w[(Fo-Fc)_2/\Sigma w[(Fo^2)^2]^{1/2}$

Table S2. EPR parameters of complex **2** and complex **3**

	$g_{\parallel}$	$g_{\perp}$	$A_{\parallel}$ ($10^{-4}cm^{-1}$)	α^2	β^2	γ^2	$K_{\parallel}$	$K_{\perp}$	K	f (cm^{-1})
2	2.260±0.001	2.060±0.004	180.26±0.03	0.833	1.080	1.256	0.757	0.651	0.323	165
3	2.371±0.002	2.055±0.006	143.76±0.06	0.818	0.928	1.124	0.898	0.741	0.363	125

$A_{\parallel}$ in 10^{-4} cm^{-1}. f in cm^{-1} $\alpha^2 = A_{\parallel}/0.036 + (g_{\parallel} - 2.0023) + 3/7\ (g_{\perp} - 2.0023) + 0.04$. $K_{\parallel} = \alpha^2\beta^2$ and $K_{\perp} = \alpha^2\gamma^2$, $K_{\parallel}^2 = (g_{\parallel} - 2.0023)\ \Delta E\ (d_{xy} - d_{x^2-y^2}) / 8\lambda_0)$, $K_{\perp}^2 = (g_{\perp} - 2.0023)\ \Delta E\ (d_{xz,yz} - d_{x^2-y^2}) / 2\lambda_0)$, $K = A_{iso}/P\beta^2 + (g_{av} - 2.0023)/\beta^2$.

Table S3. Calculated bond distance and bond angle for $[Cu^{II}L(OOH)]^+$ by TDDFT calculation

$[(LCu^{II}OOH]^+$			
Cu(1)-N(1)	2.031(6)	N(1)-Cu(1)-N(2)	90.3
Cu(1)-N(2)	2.062(8)	N(1)-Cu(1)-O(1)	73.6
Cu(1)-O(1)	2.286(5)	N(1)-Cu(1)-O(2)	135.4
Cu(1)-O(2)	1.833(4)	N(2)-Cu(1)-O(1)	74.9
O(2)-O(3)	1.380(1)	N(2)-Cu(1)-O(2)	133.1
		O(1)-Cu(1)-O(2)	121.0